



OPEN

# JNK2-MMP-9 axis facilitates the progression of intracranial aneurysms

Ryota Ishibashi<sup>1,2</sup>, Masahiko Itani<sup>1,3,4</sup>, Akitsugu Kawashima<sup>5</sup>, Yoshiki Arakawa<sup>1</sup> & Tomohiro Aoki<sup>1,3,4</sup>✉

Intracranial aneurysm (IA) can cause subarachnoid hemorrhage or some other hemorrhagic stroke after rupture. Because of the poor outcome in spite of the intensive medical care after the onset of hemorrhage, the development of a novel therapeutic strategy like medical therapy to prevent the progression of the disease becomes a social need. As the reduction of arterial stiffness due to the degeneration of the extracellular matrix via Matrix Metalloproteinases (MMPs) becomes one of the central machineries leading to the progression of IAs through a series of studies, factors regulating the expression or the activity of MMPs could be a therapeutic target. In the present study, specimens from human IA lesions and the animal model of IAs were used to examine the expression of c-Jun N-terminal kinase (JNK) which might exacerbate expressions of MMPs in the lesions to weaken arterial walls resulting in the progression of the disease. In some human IA lesions examined, the expression of p-JNK, the activated form of JNK, could be detected mostly in the medial smooth muscle cells. In IA lesions induced in rats, the activation of JNK was induced during the progression of the disease and accompanied with the activation of downstream transcriptional factor c-Jun and importantly with the expression of MMP-2 or -9. The genetic deletion of *Jnk2*, not *Jnk1*, in mice significantly prevented the incidence of IAs with the suppression of the expression of MMP-2 or MMP-9. These results combined together have suggested the crucial role of JNK in the progression of IAs through regulating the expression of MMPs. The results from the present study provides the novel insights about the pathogenesis of IA progression and also about the therapeutic target.

The outcome of subarachnoid hemorrhage (SAH) mainly due to rupture of intracranial aneurysm (IA) is still poor despite of the technical advancement in medical treatment and the intensive care<sup>1-4</sup>. Considering such a poor outcome of SAH once after the onset, the development of the novel therapeutic strategy to prevent the initiation, the progression and the rupture of IAs is socially demanded. For this purpose, the machineries regulating the pathogenesis of IAs should be clarified to identify a therapeutic target.

As the degenerative changes of vascular walls, i.e. most typically the loss of extracellular matrix (ECM) in arterial walls, becomes the histopathological feature of IA lesions<sup>5,6</sup>, the machineries regulating the degenerative changes of ECM presumably function in situ and could be a therapeutic target. Previous studies using human specimens from cases with IAs or animal model of IAs have highlighted the role of chronic inflammation in the pathogenesis of IAs<sup>7-14</sup>. In the process leading to the formation and the enlargement of IAs in inflammatory microenvironment of the disease, the crucial contribution of matrix metalloproteinases (MMPs), especially MMP-2 and MMP-9, to the degenerative changes of affected vascular walls in the lesions has been clarified<sup>14,15</sup>. However, the precise molecular mechanisms regulating the degenerative changes of vascular walls during the development of IAs remain to be elucidated.

Previous experimental studies about abdominal aortic aneurysm (AAA) have demonstrated the crucial role of JNK signaling in the progression of the disease<sup>16</sup>. The activation of JNK assessed by the phosphorylation of this kinase was detected in Western blot analyses using the lysates from AAA lesions compared with ones from controls<sup>16</sup>. Also, the expression of the phosphorylated form of JNK was well co-localized with that of MMP-9 in

<sup>1</sup>Department of Neurosurgery, Kyoto University Graduate School of Medicine, Kyoto, Japan. <sup>2</sup>Department of Neurosurgery, Medical Research Institute KITANO HOSPITAL, PIIF Tazuke-Kofukai, Osaka, Japan. <sup>3</sup>Department of Pharmacology, The Jikei University School of Medicine, 3-25-8 Nishi-Shinbashi, Minato-ku, Tokyo 105-8461, Japan. <sup>4</sup>Department of Molecular Pharmacology, National Cerebral and Cardiovascular Center, Osaka, Japan. <sup>5</sup>Department of Neurosurgery, Tokyo Women's Medical University Yachiyo Medical Center, Chiba, Japan. ✉email: tomoaoki@jikei.ac.jp

immunohistochemistry<sup>16</sup>. In cultured vascular smooth muscle cells, macrophages or ex vivo culture from human lesions, the proteinase activity of MMP-2 or MMP-9 was detected in gelatin zymography, which was significantly suppressed by the specific inhibitor for JNK, SP600125, or by the genetic deletion of JNK2<sup>16</sup>, suggesting the role of JNK signaling in the activation of MMPs. In animal AAA models induced by CaCl<sub>2</sub>, the pharmacological inhibition of JNK suppressed not only the incidence or the enlargement of the lesions but also regressed the lesions once induced through suppressing tissue destruction via the activity of MMPs and also facilitating the tissue repair via lysyl oxidase or prolyl 4-hydroxylase<sup>16</sup>. In other study using RNAi to knock down JNK expression, RNAi-induced knock down of *JNK* significantly suppressed the expression of *Lysyl oxidase* in cultured vascular smooth muscle cells and consistently prevented the degenerative change of the elastic lamina in AAA model of rats<sup>17</sup>, supporting the role of JNK signaling in tissue repair. Above previous studies have suggested the role of JNK signaling during the development of vascular disease through regulating tissue destruction.

In IAs, the previous study using human specimens has demonstrated the activation of JNK in vascular smooth muscle cells in the lesions through immunohistochemistry for the phosphorylation of JNK and its downstream factor, the phosphorylated form of c-Jun<sup>18</sup>, indicating the role of JNK signaling in the pathogenesis of IAs as in AAA. However, whether JNK signaling indeed mediates the pathogenesis of IAs through regulating tissue destruction remains to be elucidated.

## Materials and methods

### Study approval

The use of human samples in the present research was approved by the local ethical committee at Kyoto University Graduate School of Medicine (#R0456) and at National Cerebral and Cardiovascular Center (#M29-050, #R20126, #R20126-1, #20126-2, #20126-3, #20126-4) where samples were analyzed and Tokyo Women's Medical University Yachiyo Medical Center (#4106) where samples were prepared with written informed consent from each case. All of the experiments using human specimens was performed in accordance with the Declaration of Helsinki and the relevant guidelines/regulations.

All of the following experiments using animals, including animal care and use, complied with the National Institute of Health's Guide for the Care and Use of Laboratory Animals (ARRIVE guidelines (<https://arriveguidelines.org>)), and all experiments were performed in accordance with relevant guidelines and regulations. All of the experiments using animals were approved by the Institutional Animal Care and Use Committee of Kyoto University Graduate School of Medicine (Approval Number #050172), National Cerebral and Cardiovascular Center (Approval Number #19036, #20003, #21004, #22012), and Jikei University School of Medicine (Approval Number #2023-004). Also, all experiments about recombinant DNA experiment were approved by the Institutional Biosafety Committee of Kyoto University Graduate School of Medicine (Approval Number #MedKyo06516).

### Human specimen and immunohistochemistry

Human IA samples were dissected during microsurgical clipping of unruptured IAs with the written informed consent. Dissected specimen was fixed in formalin solution and embedded in paraffin. 4- $\mu$ m thick slices were then prepared for immunohistochemical analysis. After de-paraffinization and blocking with 3% donkey serum (#AB\_2337258, Jackson ImmunoResearch, West Grove, PA), slices were incubated with primary antibodies followed by incubation with secondary antibodies conjugated with fluorescence dye. Finally, fluorescent images were acquired on a confocal fluorescence microscope system (LSM880, Carl Zeiss, Oberkochen, Germany).

Primary antibodies used were as follows; mouse monoclonal anti-smooth muscle  $\alpha$ -actin antibody (clone 1A4, #14-9760-82, Thermo Fisher Scientific, Waltham, MA), rabbit monoclonal anti-p-APK/JNK (T183/Y185) antibody (#4668S, Cell Signaling Technology, Danvers, MA).

Secondary antibodies used were as follows; Alexa Fluor 488-conjugated donkey anti-mouse IgG H&L antibody (#A21202, Thermo Fisher Scientific), Alexa Fluor 647-conjugated donkey anti-rabbit IgG H&L antibody (#A31573, Thermo Fisher Scientific).

### Rodent IA models and histological analysis of induced IA lesions

7 week-old male Sprague–Dawley rats were purchased from Japan SLC (Shizuoka, Japan). Mice deficient in *Jnk1* (B6.129S1-Mapk8tm1Flv/J) or *Jnk2* (B6.129-Mapk9tm1.1Rjd/J) were purchased from The Jackson Laboratory (Bar Harbor, Maine, ME) and backcrossed with C57BL/6NcrSlc (Japan SLC, Shizuoka, Japan). Animals were maintained on a light/dark cycle of 12 h/12 h, and had a free access to chow and water.

To induce IA, under general anesthesia by the intraperitoneal injection of pentobarbital sodium (50 mg/kg, Somnopenyl, Kyoritsu Seiyaku Corporation, Tokyo, Japan) and/or the inhalation of Isoflurane (induction; 5.0%, maintenance; 1.5–2.0%, #IYESC-0001, Pfizer Inc., New York, NY), 7-week-old male rats or mice were subjected to ligation of the left carotid artery and systemic hypertension, achieved by the combination of a high salt diet and ligation of the left renal artery.

Immediately after surgical manipulations, animals were fed the food containing 8% sodium chloride and 0.12% 3-aminopropionitrile (#A0408, Tokyo Chemical Industry, Tokyo, Japan), an inhibitor of lysyl oxidase that catalyzes the cross-linking of collagen and elastin. At one or three in rats and five months in mice after the surgical manipulation, systolic blood pressure was measured by a tail-cuff method. Animals were then deeply anesthetized by intraperitoneal injection of the lethal dose of pentobarbital sodium (200 mg/kg, Somnopenyl, Kyoritsu Seiyaku Corporation) or the inhalation of Isoflurane (5.0%, #IYESC-0001, Pfizer Inc.), and transcardially perfused with 4% paraformaldehyde solution. The bifurcation site of anterior cerebral artery—olfactory artery including the induced IA lesion was stripped, and serial frozen sections were then made.

## Immunohistochemistry of IA lesions induced in animals

5-um-thick frozen sections were prepared from dissected IA lesions. After blocking with 3% donkey serum (#AB\_2337258, Jackson ImmunoResearch), slices were incubated with primary antibodies followed by incubation with secondary antibodies conjugated with a fluorescence dye. Finally, fluorescent images were acquired on a fluorescence microscope system (BX51N-34-FL-1, Olympus).

Primary antibodies used were as follows; rabbit polyclonal anti-pJNK antibody (#9251, Cell Signaling), rabbit polyclonal anti-JNK1 antibody (#sc-571, Santa Cruz Biotechnology, Dallas, Texas), rabbit polyclonal anti-phosphorylated c-Jun antibody (#9261, Cell Signaling), rabbit polyclonal phosphorylated ATF-2 antibody (#9221, Cell Signaling), rabbit polyclonal anti-MMP-2 antibody (#sc-10736, Santa Cruz Biotechnology), goat polyclonal anti-MMP-9 antibody (#sc-6840, Santa Cruz Biotechnology), mouse monoclonal anti-smooth muscle  $\alpha$ -actin antibody (clone 1A4, #14-9760-82, Thermo Fisher Scientific).

Secondary antibodies used were as follows; Alexa Fluor 488-conjugated donkey anti-rabbit IgG H&L antibody (#A21206, Thermo Fisher Scientific), Alexa Fluor 488-conjugated donkey anti-goat IgG H&L antibody (#A11055, Thermo Fisher Scientific), Alexa Fluor 594-conjugated donkey anti-mouse IgG H&L antibody (#A21203, Thermo Fisher Scientific), Alexa Fluor 594-conjugated donkey anti-rabbit IgG H&L antibody (#A21207, Thermo Fisher Scientific), and Alexa Fluor 594-conjugated donkey anti-goat IgG H&L antibody (#A11058, Thermo Fisher Scientific).

## Western blot analysis

Whole cell lysate from the ring of Willis was prepared by a RIPA buffer (#R0278, Sigma-Aldrich, St. Louis, MI) supplemented with proteinase and phosphatase inhibitors (#04693159001 and #4906837001, Roche Diagnostics, Basel, Switzerland). Protein concentration was, then, determined by a Bicinchoninic Acid (BCA) method (#23227, Pierce BCA Protein Assay Kit, Thermo Scientific). After SDS-PAGE (Sodium dodecyl sulfate- Poly-Acrylamide Gel Electrophoresis), separated proteins were blotted to a PDVF membrane (Hybond-P, #10600058, GE healthcare, Buckinghamshire, UK) and blocked with an ECL plus blocking agent (#RPN2125, GE healthcare). The membranes were then incubated with primary antibodies followed by incubation with an anti-IgG antibody conjugated by horseradish peroxidase (anti-mouse IgG, #NA931V; anti-rabbit IgG, #NA934V, GE healthcare). Finally, the signal was detected by a chemiluminescent reagent (ECL Prime Western Blotting Detection System, #RPN2236, GE healthcare).  $\alpha$ -Tubulin was served as an internal control.

Primary antibodies used in Western Blot analysis were as follows; rabbit polyclonal anti-pJNK antibody (#9251, Cell Signaling), rabbit polyclonal anti-JNK1 antibody (#sc-571, Santa Cruz Biotechnology), and mouse monoclonal anti- $\alpha$ -tubulin antibody (clone DM1A, #T6199, Sigma-Aldrich).

## Gelatin zymography

Total protein from the whole Willis ring was purified by a Bio-Plex Cell Lysis Kit (Bio-Rad, Hercules, CA) according to the manufacturer's directions. One hundred micrograms of protein was used in each reaction. Gelatin zymography was performed using a Gelatin Zymo-Electrophoresis Kit (Primary Cell, Sapporo, Japan) according to the manufacturer's directions.

## Statistics

Data are shown as mean  $\pm$  s.e.m. Differences between the 2 groups were examined using the non-parametric Mann–Whitney test. Statistical comparisons between more than 2 groups were conducted using the Kruskal–Wallis test followed by the Steel test, or the Steel–Dwass test. The incidence of IAs among groups was examined by the Fisher's Exact Test. A p value smaller than 0.05 was defined as statistically significant. Statistical analyses were performed with JMP software (version 8.0, SAS Institute, Cary, NC).

## Results

### The activation of JNK in human IA lesions

We first examined whether JNK was phosphorylated and activated in human IA lesions in immunohistochemistry by using specimens harvested from human cases with unruptured IAs (Fig. 1A). We stained slices from total 6 cases and among them the positive signals for the phosphorylated form of JNK reflecting the activation of this factor could be observed in all slices to a certain extent (Fig. 1A). The signals for the phosphorylated form of JNK was well co-localized with those for nuclei (Fig. 1A), suggesting the nuclear translocation of activated JNK. Here, because antibodies specifically recognize each isoform of JNK, JNK1 and JNK2, were not available, whether only a specific isoform is activated or not could not be clarified. Most of the cells positive for the phosphorylated form of JNK was also positive for the smooth muscle cell marker, SMA, in immunohistochemistry (Fig. 1B), suggesting the activation of JNK mostly in medial smooth muscle cells in IA lesions.

### The activation of JNK signaling cascade in IA lesions of rats

To corroborate the precise contribution of JNK signaling cascade to the pathogenesis of IAs, the animal models previously established<sup>9,19,20</sup> were used. Whether the activation of JNK in IA lesion could be observed was examined in immunohistochemistry to confirm the reproducibility of the findings in human specimens (Fig. 1). As a result, the expression of the phosphorylated form of Jnk in the lesions was indeed reproduced and confirmed to be induced, as expected, at one or three months after the experimental induction of IA lesions in rats<sup>19</sup> (Fig. 2A). The activation of Jnk, evidenced by the increase in the phosphorylation of this kinase, was also supported by western blot analyses (Fig. 2B and C, Sup. Fig. 1A). In addition, most of the signals for the phosphorylated form of Jnk was also positive for the smooth muscle cell marker, SMA, in immunohistochemistry (Fig. 2D), confirming the activation of JNK in medial smooth muscle cells of the lesions as in human.

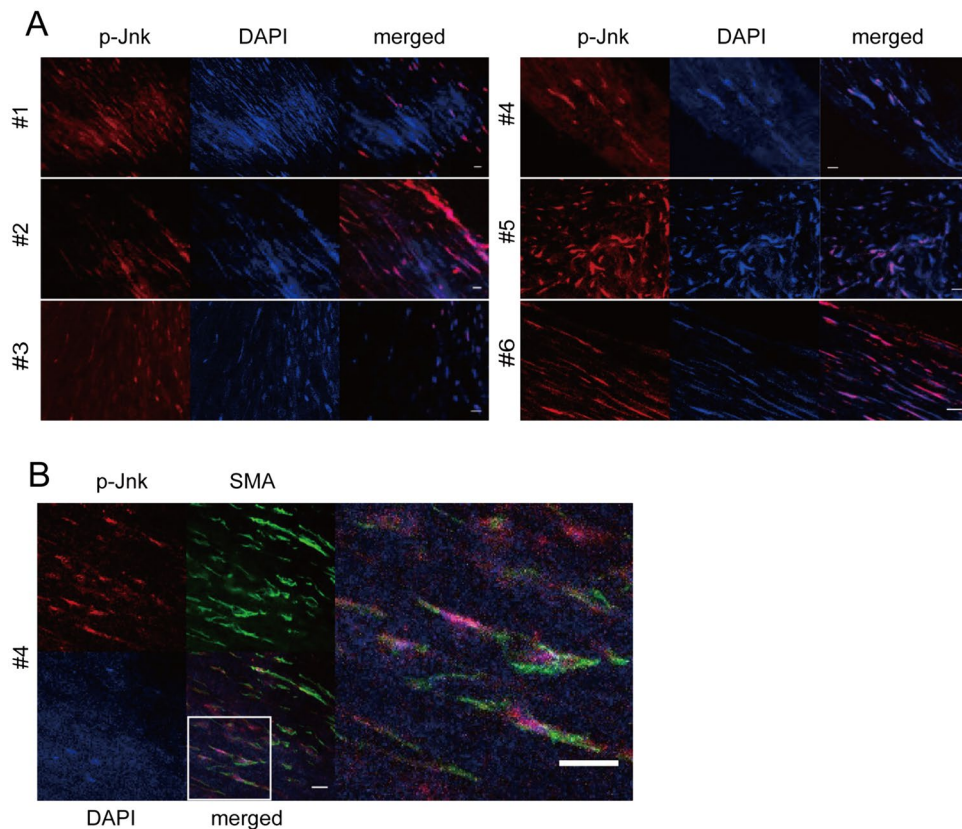


**Figure 1.** Expression of the phosphorylated form of JNK in human intracranial aneurysm lesions. Expression of the phosphorylated form of JNK (p-JNK) mostly in medial smooth muscle cells of intracranial aneurysm (IA) lesions from 6 cases (from #1 to #6). IA lesions were harvested and then subjected to immunohistochemical analyses. The images of immunofluorescent staining of IA lesions for p-JNK (red in (A) and (B)), the marker for smooth muscle cells,  $\alpha$ -smooth muscle actin (SMA in (B), green), nuclear staining by DAPI (blue), and merged images are shown. The magnified image corresponding to the white square is shown on the right. Scale bar: 10  $\mu$ m.

Referencing the potential of JNK to the induction of MMPs, whether JNK signaling cascade was indeed driven in IA lesions to facilitate MMP expression was then examined in immunohistochemistry. In IA lesions, most of the signals for the phosphorylated form of Jnk was also positive for ones reflecting the activation of the downstream transcription factor, c-Jun or Atf, in immunohistochemistry (Fig. 3A and B), confirming the activation of downstream signaling cascade of JNK in the lesions. Importantly, the signals for the phosphorylated form of Jnk was also positive for tissue destructive MMPs, Mmp-2 or Mmp-9 (Fig. 3C and D), as hypothesized.

### The contribution of JNK2 to the induction or the enlargement of IAs

To clarify the involvement of JNK function in the pathogenesis of IAs, mice deficient in each isoform of JNK were used and subjected to the animal model of IAs<sup>9,20</sup>. The deletion of both *Jnk1* and *Jnk2* in mice could suppress the incidence and the size of IAs (Fig. 4A–C). However, the suppressive effect of the deletion of only *Jnk2*, not *Jnk1*, on both the incidence and the enlargement of the lesions reached the pre-configured statistical significance (Fig. 4A–C) without influencing the systemic blood pressure (Fig. 4D), supporting the predominant role of JNK2 signaling in IA pathogenesis. In mice deficient in *Jnk2*, the expressions of both Mmp-2 and Mmp-9 were remarkably suppressed (Fig. 5A), indicating the Jnk-dependent induction of MMPs. Consistently, genetic deletion of *Jnk2* in mice suppressed the activity of MMP-9 in gelatin zymography which examines the activity of MMP-2 or -9 (Fig. 5B, Sup. Fig. 1B).

These results combined together have suggested the role of JNK2 signaling cascade in the induction or the enlargement of IAs through regulating MMP expression.

### Discussion

Through a series of studies about the contribution of JNK to diseases, JNK signaling might contribute to various vascular diseases as one of the common disease-regulating cascades. In addition to IAs and AAA<sup>16,21,22</sup>, the involvement of JNK signaling in the pathogenesis of Kawasaki disease has also been demonstrated<sup>23</sup>. In *Candida albicans*-induced mouse model of Kawasaki disease, the activation of JNK visualized by the immunohistochemistry for the phosphorylated form of JNK was remarkably induced in vascular smooth muscle cells present in the

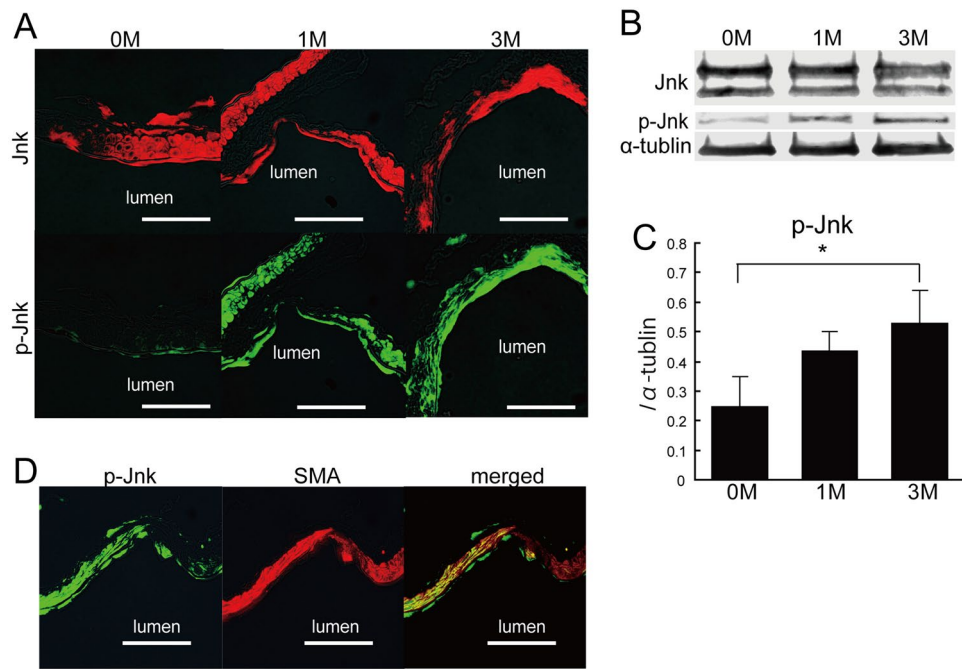


**Figure 2.** Activation of Jnk in intracranial aneurysm lesions induced in rats. Expression of the phosphorylated form of Jnk (p-Jnk) mainly in medial smooth muscle cells of intracranial aneurysm (IA) lesions induced in rats. At 1 (1M) or 3 (3M) months after the induction in rats, IA lesions were harvested and then subjected to immunohistochemical analyses. The images of immunofluorescent staining of IA lesions for total Jnk (red in (A)), p-Jnk (green in (A) and (D)), the marker for smooth muscle cells,  $\alpha$ -smooth muscle actin (SMA in (D), red), and merged images are shown. Scale bar: 50  $\mu$ m. The representative images of western blot analyses and the results from densitometry analyses are shown in (B and C). Bars in C represent mean  $\pm$  s.e.m. Statistical comparison was done by the Kruskal–Wallis test.

lesions affecting aorta<sup>23</sup>. The pharmacological inhibition of JNK by the specific inhibitor, SP600125, significantly suppressed the incidence of the disease and also the size of the lesions once induced<sup>23</sup>, again suggesting the crucial role of JNK signaling in vascular diseases. Considered with the similar pathological feature of IAs, AAA and Kawasaki disease; destructive remodeling of affected arterial walls, JNK expressed mainly at vascular smooth muscle cells functions to facilitate the initiation or the progression of these diseases through the degeneration of ECM and resultant weakness of arterial walls at least partially via MMP induction. In this sense, JNK itself or a factor to activate or mediate JNK signaling cascade could be a therapeutic target for various vascular diseases including IAs with destructive remodeling.

In diseases other than vascular diseases discussed in the above section, the central role of JNK cascade in the pathogenesis and also the potential of JNK inhibitors as a therapeutic drug to a disease have also been demonstrated. These diseases include a wide range of diseases like cancers, metabolic diseases, neurodegenerative diseases or infectious diseases<sup>24–32</sup>. Thereby, the findings from the present study and studies targeting various

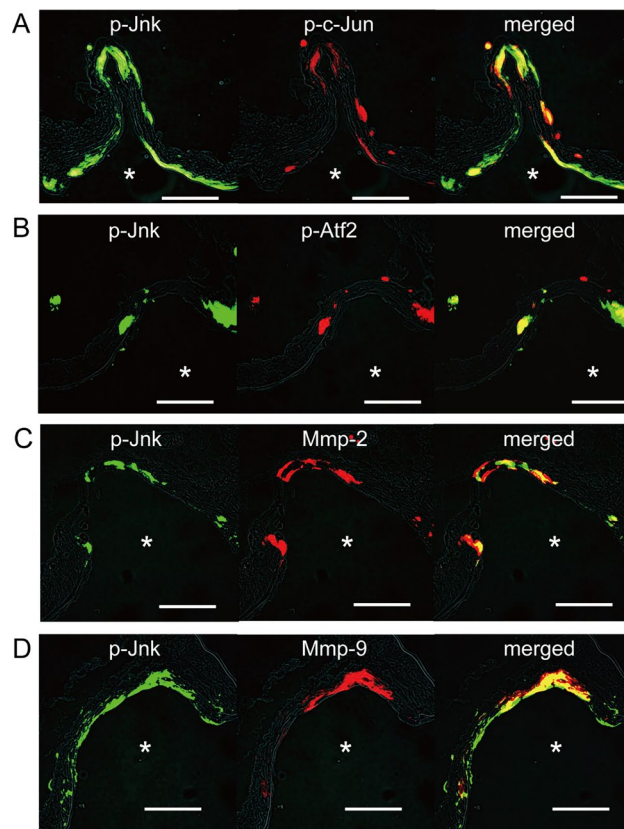


**Figure 3.** Co-expression of the phosphorylated form of Jnk and downstream factors in intracranial aneurysm lesions induced in rats. Co-expression of the phosphorylated form of Jnk (p-Jnk) and downstream factors mostly in intracranial aneurysm (IA) lesions induced in rats. IA lesions were harvested at 3 months after the induction in rats and then subjected to immunohistochemical analyses. The images of immunofluorescent staining of IA lesions for p-Jnk (green), the phosphorylated form of c-Jun (red in (A)), the phosphorylated form of Atf (red in (B)), Mmp-2 (red in (C)), Mmp-9 (red in (D)), and merged images are shown. Scale bar: 50  $\mu$ m. \* indicates lumen.

disease could each other contribute to the understanding of the pathogenesis and to the development of therapeutic drugs.

JNK consists of three isoforms, JNK1, JNK2 and JNK3<sup>33</sup>. Among them, JNK3 differently behaves and has a unique function from two other isoforms presumably because of its relatively specific expression pattern in tissues like brain. Instead, both JNK1 and JNK2 can ubiquitously be detected in various tissues and also phosphorylate same downstream factors like c-Jun upon activation. JNK1 and JNK2 is, thus, considered to redundantly function and to be able to compensate each other. However, the experimental studies using some disease models and applying the genetic deletion of *Jnk1* or *Jnk2* to animals has consistently revealed the distinct contribution of these two isoforms to the pathogenesis<sup>16,33</sup>. In the present study, the genetic deletion of *Jnk2*, not of *Jnk1*, predominantly suppressed the incidence of IAs as in other studies, again supporting the functional diversities between JNK1 and JNK2. The precise mechanisms why these two isoforms differently behave in microenvironment of

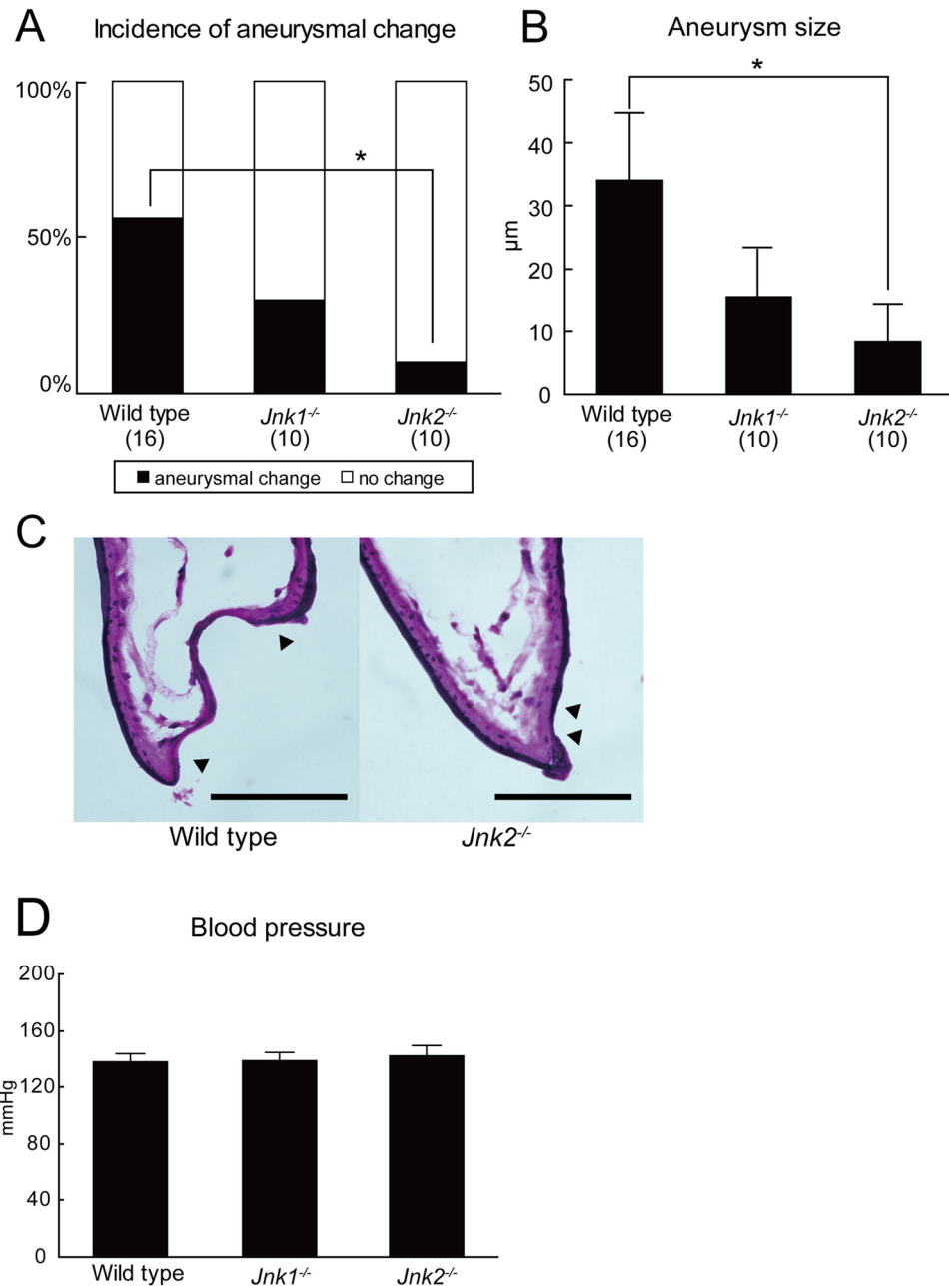


**Figure 4.** Contribution of JNK to the induction or the enlargement of intracranial aneurysm lesions in mice. Suppressive effect of the genetic deletion of *Jnk1* and *Jnk2* on the incidence of intracranial aneurysm (IA) lesions or the size of induced lesions in mice. Wild type mice, ones deficient in *Jnk1* or *Jnk2* was subjected to IA induction and the incidence of IAs or the size of induced lesions was histopathologically assessed after Elastica van Gieson staining. Number of animals used is shown in the parenthesis. Statistical analyses was done by using the Fisher's Exact test in (A) or the Kruskal–Wallis Test in (B). \* $p < 0.05$ . The representative images of histopathological analyses are shown in (C). Arrow heads in (C) indicate the border of IA lesion. Scale bar: 50  $\mu\text{m}$ . Systolic blood pressure was measured by tail-cuff method before sacrifice and its value is shown in (D). Bars indicate mean  $\pm$  s.e.m.

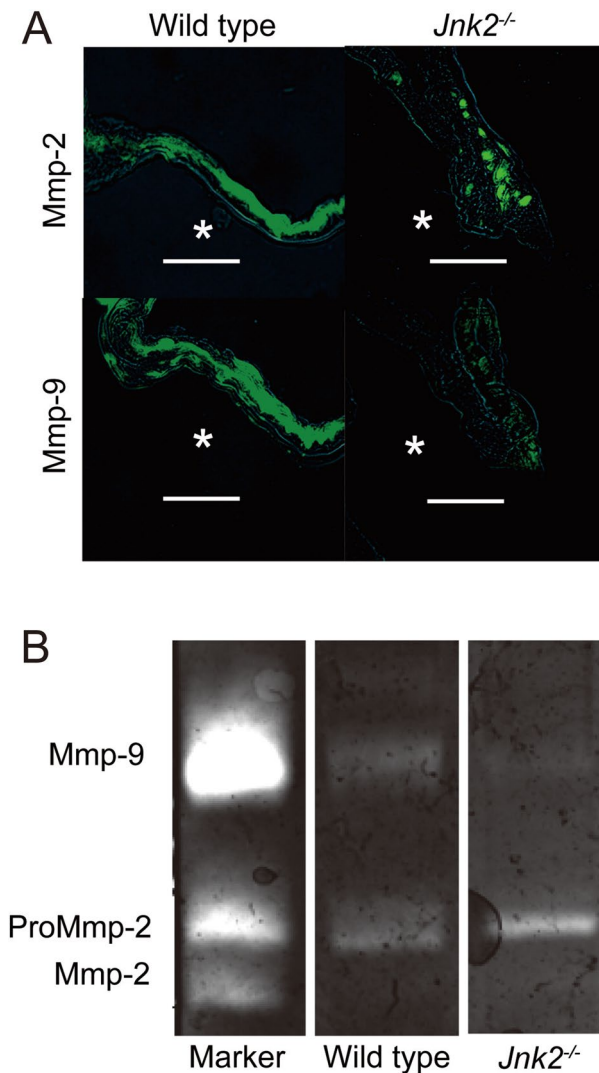


**Figure 5.** JNK2-dependent expression and activation of Mmp-9 in intracranial aneurysm lesions in mice. Suppressive effect of the genetic deletion of *Jnk2* on the expression of Mmp-2 or Mmp-9 in intracranial aneurysm (IA) lesions induced in mice (A). The slices from IA lesion induced in wild type mice or ones deficient in *Jnk2* was subjected to immunohistochemical analyses. The images of immunofluorescent staining of IA lesions for Mmp-2 or Mmp-9 are shown. Scale bar: 50  $\mu$ m. The representative images from 3 independent experiments by the gelatin zymography to examine the influence of the genetic deletion of *Jnk2* in the activity of Mmp-2 or -9 are also shown in (B). \* indicates lumen.

diseases in spite of the ubiquitous and the similar expression pattern, however, remains to be elucidated. Also, the development and the usage of potent and highly-selective isotype-specific inhibitors of JNK, not non-specific JNK inhibitors, is ideal.

### Data availability

All of the data in the present study is available from the corresponding author upon reasonable request.

Received: 22 May 2024; Accepted: 16 August 2024

Published online: 21 August 2024

### References

1. Brisman, J. L., Song, J. K. & Newell, D. W. Cerebral aneurysms. *N. Engl. J. Med.* **355**(9), 928–939 (2006).
2. Lawton, M. T. & Vates, G. E. Subarachnoid hemorrhage. *N. Engl. J. Med.* **377**(3), 257–266 (2017).
3. van Gijn, J., Kerr, R. S. & Rinkel, G. J. Subarachnoid haemorrhage. *Lancet* **369**(9558), 306–318 (2007).
4. Wermer, M. J., Kool, H., Albrecht, K. W. & Rinkel, G. J. Subarachnoid hemorrhage treated with clipping: Long-term effects on employment, relationships, personality, and mood. *Neurosurgery* **60**(1), 91–7 (2007).
5. Kataoka, K. *et al.* Structural fragility and inflammatory response of ruptured cerebral aneurysms. A comparative study between ruptured and unruptured cerebral aneurysms. *Stroke* **30**(7), 1396–401 (1999).



6. Frosen, J. *et al.* Remodeling of saccular cerebral artery aneurysm wall is associated with rupture: Histological analysis of 24 unruptured and 42 ruptured cases. *Stroke* **35**(10), 2287–2293 (2004).
7. Aoki, T. *et al.* Impact of monocyte chemoattractant protein-1 deficiency on cerebral aneurysm formation. *Stroke* **40**(3), 942–951 (2009).
8. Aoki, T. *et al.* NF-kappaB is a key mediator of cerebral aneurysm formation. *Circulation* **116**(24), 2830–2840 (2007).
9. Aoki, T. *et al.* Prostaglandin E2-EP2-NF-kappaB signaling in macrophages as a potential therapeutic target for intracranial aneurysms. *Sci. Signal.* **10**(465), eaah6037 (2017).
10. Shimizu, K., Kushamae, M., Mizutani, T. & Aoki, T. Intracranial aneurysm as a macrophage-mediated inflammatory disease. *Neurol. Med. Chir. (Tokyo)* **59**(4), 126–132 (2019).
11. Turjman, A. S., Turjman, F. & Edelman, E. R. Role of fluid dynamics and inflammation in intracranial aneurysm formation. *Circulation* **129**(3), 373–382 (2014).
12. Tulamo, R., Frosen, J., Hernesniemi, J. & Niemela, M. Inflammatory changes in the aneurysm wall: A review. *J. Neurointerv. Surg.* **10**(Suppl 1), i58–i67 (2018).
13. Frosen, J., Cebral, J., Robertson, A. M. & Aoki, T. Flow-induced, inflammation-mediated arterial wall remodeling in the formation and progression of intracranial aneurysms. *Neurosurg. Focus* **47**(1), E21 (2019).
14. Kushamae, M. *et al.* Involvement of neutrophils in machineries underlying the rupture of intracranial aneurysms in rats. *Sci. Rep.* **10**(1), 20004 (2020).
15. Aoki, T., Kataoka, H., Morimoto, M., Nozaki, K. & Hashimoto, N. Macrophage-derived matrix metalloproteinase-2 and -9 promote the progression of cerebral aneurysms in rats. *Stroke* **38**(1), 162–169 (2007).
16. Yoshimura, K. *et al.* Regression of abdominal aortic aneurysm by inhibition of c-Jun N-terminal kinase. *Nat. Med.* **11**(12), 1330–1338 (2005).
17. Carney, S., Broekelmann, T., Mecham, R. & Ramamurthi, A. JNK2 gene silencing for elastic matrix regenerative repair. *Tissue Eng. A* **28**(5–6), 239–253 (2022).
18. Takagi, Y., Ishikawa, M., Nozaki, K., Yoshimura, S. & Hashimoto, N. Increased expression of phosphorylated c-Jun amino-terminal kinase and phosphorylated c-Jun in human cerebral aneurysms: Role of the c-Jun amino-terminal kinase/c-Jun pathway in apoptosis of vascular walls. *Neurosurgery* **51**(4), 997–1002 (2002).
19. Aoki, T., Miyata, H., Abekura, Y., Koseki, H. & Shimizu, K. Rat model of intracranial aneurysm: Variations, usefulness, and limitations of the Hashimoto model. *Acta Neurochir. Suppl.* **127**, 35–41 (2020).
20. Morimoto, M. *et al.* Mouse model of cerebral aneurysm: Experimental induction by renal hypertension and local hemodynamic changes. *Stroke* **33**(7), 1911–1915 (2002).
21. DiMusto, P. D. *et al.* Increased JNK in males compared with females in a rodent model of abdominal aortic aneurysm. *J. Surg. Res.* **176**(2), 687–695 (2012).
22. Camardo, A., Seshadri, D., Broekelmann, T., Mecham, R. & Ramamurthi, A. Multifunctional, JNK-inhibiting nanotherapeutics for augmented elastic matrix regenerative repair in aortic aneurysms. *Drug Deliv. Transl. Res.* **8**(4), 964–984 (2018).
23. Yoshikane, Y. *et al.* JNK is critical for the development of *Candida albicans*-induced vascular lesions in a mouse model of Kawasaki disease. *Cardiovasc. Pathol.* **24**(1), 33–40 (2015).
24. Yan, H., He, L., Lv, D., Yang, J. & Yuan, Z. The role of the dysregulated JNK signaling pathway in the pathogenesis of human diseases and its potential therapeutic strategies: A comprehensive review. *Biomolecules* **14**(2), 243 (2024).
25. Chen, J. *et al.* The roles of c-Jun N-terminal kinase (JNK) in infectious diseases. *Int. J. Mol. Sci.* **22**(17), 9640 (2021).
26. Hepp Rehfeldt, S. C., Majolo, F., Goettert, M. I. & Laufer, S. c-Jun N-terminal kinase inhibitors as potential leads for new therapeutics for Alzheimer's diseases. *Int. J. Mol. Sci.* **21**(24), 9677 (2020).
27. Yung, J. H. M. & Giacca, A. Role of c-Jun N-terminal kinase (JNK) in obesity and type 2 diabetes. *Cells* **9**(3), 706 (2020).
28. Busquets, O. *et al.* Role of c-Jun N-terminal kinases (JNKs) in epilepsy and metabolic cognitive impairment. *Int. J. Mol. Sci.* **21**(1), 255 (2019).
29. Shvedova, M., Anfinogenova, Y., Atochina-Vasserman, E. N., Schepetkin, I. A. & Atochina, D. N. c-Jun N-terminal kinases (JNKs) in myocardial and cerebral ischemia/reperfusion injury. *Front. Pharmacol.* **9**, 715 (2018).
30. Bubici, C. & Papa, S. JNK signalling in cancer: In need of new, smarter therapeutic targets. *Br. J. Pharmacol.* **171**(1), 24–37 (2014).
31. Tilg, H. & Moschen, A. R. Inflammatory mechanisms in the regulation of insulin resistance. *Mol. Med.* **14**(3–4), 222–231 (2008).
32. Heasley, L. E. & Han, S. Y. JNK regulation of oncogenesis. *Mol. Cells* **21**(2), 167–173 (2006).
33. Bode, A. M. & Dong, Z. The functional contrariety of JNK. *Mol. Carcinog.* **46**(8), 591–598 (2007).

## Author contributions

T. A. got the grant. R. I., T. A. and Y.A. planned the experiments. A. K. acquired human specimen. R. I., M. I. and T. A. acquired the data. R. I., M. I., Y. A. and T. A. interpreted the data. R. I., Y. A. and T.A. wrote the manuscript. All authors read and approved the final manuscript.

## Funding

This work was supported by Grant-in-Aid for Scientific Research from the Ministry of Education, Culture, Sports, Science and Technology of Japan (grant ID; #24890097, #26861145, #20K09381 and #22H00584, T. A.).

## Competing interests

The authors declare no competing interests.

## Additional information

**Supplementary Information** The online version contains supplementary material available at <https://doi.org/10.1038/s41598-024-70493-5>.

**Correspondence** and requests for materials should be addressed to T.A.

**Reprints and permissions information** is available at [www.nature.com/reprints](http://www.nature.com/reprints).

**Publisher's note** Springer Nature remains neutral with regard to jurisdictional claims in published maps and institutional affiliations.

**Open Access** This article is licensed under a Creative Commons Attribution-NonCommercial-NoDerivatives 4.0 International License, which permits any non-commercial use, sharing, distribution and reproduction in any medium or format, as long as you give appropriate credit to the original author(s) and the source, provide a link to the Creative Commons licence, and indicate if you modified the licensed material. You do not have permission under this licence to share adapted material derived from this article or parts of it. The images or other third party material in this article are included in the article's Creative Commons licence, unless indicated otherwise in a credit line to the material. If material is not included in the article's Creative Commons licence and your intended use is not permitted by statutory regulation or exceeds the permitted use, you will need to obtain permission directly from the copyright holder. To view a copy of this licence, visit <http://creativecommons.org/licenses/by-nc-nd/4.0/>.

© The Author(s) 2024